An Efficient Multigrid Method for Molecular Mechanics Modeling in Atomic Solids

Jingrun Chen [1] and Pingbing Ming[2,*]

[1] *Institute of Computational Mathematics and Scientific/Engineering Computing, AMSS, Chinese Academy of Sciences, Beijing, 100190, P.R. China.*
[2] *LSEC, Institute of Computational Mathematics and Scientific/Engineering Computing, AMSS, Chinese Academy of Sciences, Beijing, 100190, P.R. China.*

Abstract. We propose a multigrid method to solve the molecular mechanics model (molecular dynamics at zero temperature). The Cauchy-Born elasticity model is employed as the coarse grid operator and the elastically deformed state as the initial guess of the molecular mechanics model. The efficiency of the algorithm is demonstrated by three examples with homogeneous deformation, namely, one dimensional chain under tensile deformation and aluminum under tension and shear deformations. The method exhibits linear-scaling computational complexity, and is insensitive to parameters arising from iterative solvers. In addition, we study two examples with inhomogeneous deformation: vacancy and nanoindentation of aluminum. The results are still satisfactory while the linear-scaling property is lost for the latter examples.

AMS subject classifications: 65B99, 65N30, 65Z05, 74G15, 74G65, 74S05

Key words: Multigrid method, Linear-scaling algorithm, Cauchy-Born rule, Nanoindentation.

1 Introduction

Molecular mechanics model is an important tool for studying static properties of atomic solids. At zero temperature (or lower temperature), the equilibrium state is obtained by minimizing the total energy subject to certain boundary condition and external loading. The most popular approach is the lattice statics proposed by Born and Huang [3]. Recent development of this method can be found in [39] and the references therein. The lattice statics has been widely used to study the equilibrium configurations and many other properties of solids. This method considers a harmonic perfect crystal with an eigendeformation as the defect, and solves the equilibrium equations arising from the minimization problem. Therefore, the solution obtained represents the equilibrium state, which may be a local minimum, a metastable state or even a global minimum.

*Corresponding author. *Email addresses:* chenjr@lsec.cc.ac.cn (J. Chen), mpb@lsec.cc.ac.cn (P.B. Ming)

In contrast, we turn to the direct minimization of the molecular mechanics model. By [11, 12, 38], the elastically deformed states are only local minima of the total energy at zero temperature. Therefore, we seek for relevant local minimum. The principal difficulty arises from the nonconvexity of the total energy. There are two sources of nonconvexity. On the one hand, the potential energy function is usually nonconvex; on the other hand, the translation invariance of the underlying crystal naturally imposes nonconvexity on the total energy even though the potential energy function is convex [18]. A crucial step for the success of the traditional minimization algorithms is to find a good initial guess, which places the crystal in the right energy well nearby the configurations of interest.

By [12], under certain stability conditions on the phonon spectra of the crystal, there is a unique local minimum of the atomistic model sitting nearby the elastically deformed state. This motivates us to employ the elastically deformed state as the initial guess for the minimization algorithms of the atomistic model. First, we solve the Cauchy-Born (CB) elasticity model over the successively refined meshes. Next we interpolate the solution to the atomic sites and take the interpolant as the initial guess for the atomistic model. Finally, the atomistic model is minimized with the given initial guess. Similar ideas can be found in many atomistic simulations of fracture and dislocation, where explicit solutions of elasticity model over the whole space, such as the solution obtained by Sin and Liebowitz [32] and the Stroh's formalism [36], are employed.

We demonstrate the efficiency of the current method by a set of representative examples. The method is applied to crystals under either homogeneous deformation or inhomogeneous deformation. For crystals under homogeneous deformation, the total CPU time scales linearly with respect to the total number of the atoms. Hence, the proposed method is a linear-scaling algorithm. For crystals under inhomogeneous deformation, the method still gives satisfactory results. The linear-scaling property is even recovered for a problem with vacancy by an additional local correction step.

It is worth mentioning that the method automatically bypasses many irrelevant local minima since the elastically deformed state is relatively smooth. It is a notorious fact that there are enormous local minima for the molecular mechanics models. For example, there are 1467 different local minima for Lennard-Jones cluster problem [9] that is closely related to the problem in study. Another interesting aspect of this method is that it is insensitive to parameters in the nonlinear iterative solvers, which may be due to the hierarchical structure of the method.

In contrast to the quasicontinuum method [34] that combines the macroscopic model and the microscopic model in a concurrent way, our method is a sequential multiscale method in the terminology of multiscale modeling and multiscale methods [4, 10].

Compared with our method, the commonly used quasistatic process also gives satisfactory results if the increment of the deformation is sufficiently small. During the process, the state obtained in the former step is taken as the initial guess of the latter step, and all the steps must be computed sequentially. In the current method, instead, the latter step can be independent of the former step since the elastic state obtained by the CB

elasticity model is employed as the initial guess.

The outline of the paper is as follows. In § 2, we describe our method and demonstrate the difficulty in solving the molecular mechanics model (MM) and the CB elasticity model. In § 3, we report three examples of the homogeneous deformation, which include one dimensional chain under tensile loading, and aluminum under tensile loading and shear loading. The tests for the inhomogeneous deformation are shown in § 4, which contains vacancy and nanoindentation. Conclusions are drawn and possible extensions are discussed in the last section.

2 Multigrid Method for the Molecular Mechanics Model

2.1 Atomistic and continuum models of crystalline solids

Under normal conditions, atoms in a crystal are arranged regularly over a lattice, which can be categorized into two types: simple lattice and complex lattice. Any lattice site $\boldsymbol{x}$ of a simple lattice takes the following form:

$$\boldsymbol{x}=\sum_{i=1}^{d}v^i\boldsymbol{e}_i+\boldsymbol{o},$$

where $\{v^i\}_{i=1}^d\in\mathbb{Z},\{\boldsymbol{e}_i\}_{i=1}^d$ are the basis vectors, d is the dimension, and $\boldsymbol{o}$ is a particular lattice site which can be taken as the origin. In principle, any lattice can be regarded as a union of congruent simple lattices [14] with shift vectors among them.

Consider a system with N atoms interacting through the potential function V, and let $\boldsymbol{f}_i$ be the external force on the i-th atom. At zero temperature, the total energy of the system can be written as a sum of the energy of each atom:

$$E^{\text{tot}}(\boldsymbol{y})=V(\boldsymbol{y}_1,\ldots,\boldsymbol{y}_N)-\sum_{i=1}^{N}\boldsymbol{f}_i\cdot\boldsymbol{y}_i,$$

where $\boldsymbol{y}_i$ is the position of the i-th atom in the deformed state. The atomic configuration is then given by the following minimization problem:

$$\{\boldsymbol{y}_1,\ldots,\boldsymbol{y}_N\}=\operatorname{argmin}E^{\text{tot}}(\boldsymbol{y}) \tag{2.1}$$

with $\boldsymbol{y}$ subject to certain boundary condition. The displacement of the i-th atom is defined as

$$\boldsymbol{u}_i=\boldsymbol{y}_i-\boldsymbol{x}_i,$$

where $\boldsymbol{x}_i$ is the position of the i-th atom in the undeformed configuration.

In the continuum model of solids, the displacement field $\boldsymbol{u}$ is a vector that is usually determined by the following variational problem:

$$I(\boldsymbol{u})=\min_{\boldsymbol{v}\in X}I(\boldsymbol{v}) \tag{2.2}$$

with

$$I(\boldsymbol{v}) = \int_\Omega \big(W(D\boldsymbol{v}(\boldsymbol{x})) - \boldsymbol{f}(\boldsymbol{x})\cdot\boldsymbol{v}(\boldsymbol{x})\big)\,\mathrm{d}\boldsymbol{x},$$

where Ω is the domain occupied by the material in the undeformed state, X is a suitable function space and W is the stored energy density that is in general a functional of the displacement gradient (or deformation gradient). In the literature of continuum mechanics, W is often obtained empirically by fitting a few experimental parameters such as the elastic moduli. A more general proposal is to obtain W from the atomistic model by the CB rule [3, 16]. For simple lattice, the CB rule works as follows. Let $\boldsymbol{F} = \boldsymbol{I} + D\boldsymbol{u}$ be the deformation gradient tensor, and $E_0(\boldsymbol{F})$ be the energy of the unit cell in the deformed lattice whose lattice vectors $\{\boldsymbol{a}_i\}_{i=1}^3$ are given by

$$\boldsymbol{a}_i = \boldsymbol{F}\boldsymbol{A}_i,$$

where $\{\boldsymbol{A}_i\}_{i=1}^3$ are lattice vectors of the undeformed lattice. The stored energy density is given by

$$W_{\mathrm{CB}}(\boldsymbol{F}) = \frac{E_0(\boldsymbol{F})}{v_0},$$

where v_0 is the volume of the unit cell in the equilibrium state. Considering a two-body potential function V_2, we write W_{CB} as

$$W_{\mathrm{CB}}(\boldsymbol{F}) = \frac{1}{2v_0}\sum_{\boldsymbol{s}} V_2(\boldsymbol{F}\boldsymbol{s}),$$

where $\boldsymbol{s}$ runs over the range of the potential function.

As an illustrative example, we consider one dimensional chain interacting through the Lennard-Jones (LJ) potential [23]:

$$V(r) = 4\left(\left(\frac{\sigma}{r}\right)^{12} - \left(\frac{\sigma}{r}\right)^{6}\right), \tag{2.3}$$

where σ is a parameter representing the atomic length scale. Considering the infinite range of interactions, we obtain the explicit expression of W_{CB} as

$$W_{\mathrm{CB}}(F) = \frac{4}{r^*}\frac{\zeta^2(6)}{\zeta(12)}\left(\frac{1}{4}|F|^{-12} - \frac{1}{2}|F|^{-6}\right), \tag{2.4}$$

where the equilibrium bond length is given by

$$r^* = \left(\frac{2\zeta(12)}{\zeta(6)}\right)^{\frac{1}{6}}\sigma$$

with the Riemann zeta function $\zeta(n) \equiv \sum_{k=1}^{\infty} k^{-n}$. The expression of the equilibrium bond length of the finite-range interaction can be found in the next section.

For the case when V is a many-body potential and the underlying lattice is a complex lattice, the definition of W_{CB} is more involved, and we are concerned with [12, 35] for details.

The stored energy density is not convex in general; see e.g., (2.4). Actually, it is not convex in certain weaker sense. To be more precise, it is not quasiconvex as proven in [2, 5,17]. This is mainly due to the periodicity of the lattice structure and the invariance of the potential function [21]. As in [5], we are concerned with the equilibrium configurations of the crystal under certain load, which are local minima of the total energy. This is usually achieved by solving the following approximation problem of (2.2):

$$I(\boldsymbol{u}_H) = \min_{\boldsymbol{v}\in X_H} I(\boldsymbol{v}),$$

where X_H is the linear finite element space with mesh size H. This yields a nonconvex minimization problem that is highly nonlinear. Such nonconvex minimization problem may well yield many physically irrelevant local minima, which may trap the minimization process.

We use Newton method, Newton-Raphson method and conjugate gradient (CG) method to solve the minimization problems arising from both the continuum and atomistic models. The choice of different solvers is due to custom and simplicity. Line search technique will be employed whenever necessary.

2.2 Difficulty in solving the atomistic and continuum models

We illustrate the difficulty in solving the atomistic and continuum models by studying one dimensional chain with $N+1$ atoms interacting through the LJ potential. We assume that the interaction range is up to the 4-th neighborhood, which will be explained later on. In this case, the equilibrium bond length is given by

$$r^* = \sqrt[6]{2}\sigma(A/B)^{1/6}$$

with $A = 1+2^{-12}+3^{-12}+4^{-12}$ and $B = 1+2^{-6}+3^{-6}+4^{-6}$.

Let the occupied interval be $[0,1]$, i.e., $Nr^* = 1$, which leads to

$$\sigma = \left[N\sqrt[6]{2}(A/B)^{1/6}\right]^{-1}.$$

The total energy is

$$E^{\mathrm{tot}}(\boldsymbol{y}) = \sum_{\ell=1}^{4}\sum_{i=2}^{N+1-\ell} V(|y_i - y_{i+\ell}|).$$

We need to solve the following minimization problem:

$$\min E^{\mathrm{tot}}(\boldsymbol{y})$$

subject to the Dirichlet boundary condition $y_1 = 0, y_{N+1} = 1+\delta$.

The stored energy density of the continuum model is given by

$$W_{\mathrm{CB}}\left(\frac{\mathrm{d}v}{\mathrm{d}x}\right)=\frac{B^2}{r^*A}\left(\left|1+\frac{\mathrm{d}v}{\mathrm{d}x}\right|^{-12}-2\left|1+\frac{\mathrm{d}v}{\mathrm{d}x}\right|^{-6}\right).$$

The corresponding CB elasticity problem (2.2) becomes

$$\min W_{\mathrm{CB}}\left(\frac{\mathrm{d}v}{\mathrm{d}x}\right)$$

subject to the Dirichlet boundary condition $v(0)=0$ and $v(1)=\delta$.

The ideal strength (stress) is the highest achievable strength of a defect-free crystal [25]. In this example, elastically deformed states are known a priori. Hence we can compute the ideal strain, the ideal strength and the stress-strain curve; see Figure 1. The ideal strain is 0.1086, which means that the atomic chain is elastically deformed when the amount of stretch is smaller than 10.86% while plastic deformation occurs after this threshold. Although elastically deformed states become mechanically unstable when the strain is greater than 10.86%, we retain these to make the ideal stress and the ideal strain more observable.

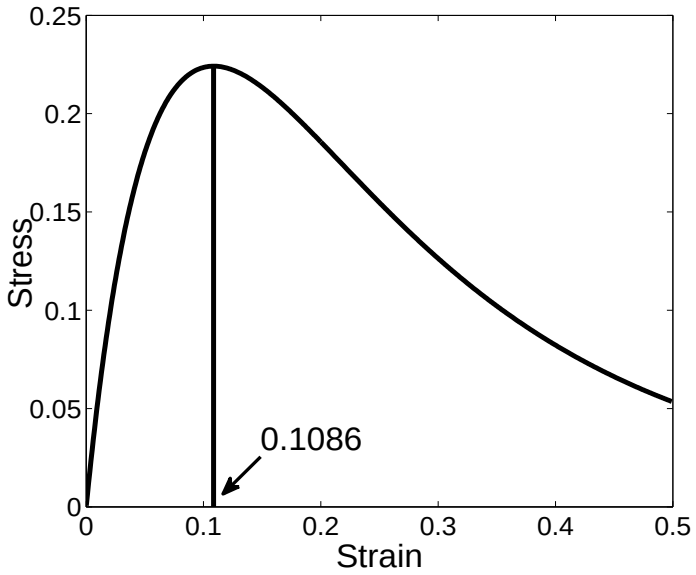

Figure 1: Stress-strain curve for elastically deformed states of one dimensional chain.

First we employ the linear finite element method to solve the CB elasticity problem. The resulting nonlinear problem is solved by Newton method with line search whose parameters are taken from [13]. The initial guess is set as zero. Denote by δ_c the numerical

ideal strain, and n the degrees of freedom (Dofs) of the discretization problem, respectively. We report δ_c in terms of n in Table 1. It is clear that δ_c is about one percent of the ideal strain when n is larger than 1000.

n	2	4	100	1024	Ideal
δ_c	.1077	.0804	.0106	.0017	0.1086

Table 1: Numerical ideal strain vs. Dofs in the continuum model.

Next we turn to MM. Since the interaction range is not restricted to the nearest neighbor and the Dirichlet boundary condition is imposed, we add certain ghost atoms to both ends of the chain to avoid the nonsmooth deformation for atoms near the boundary. The procedure is similar to the extrapolation technique employed in the construction of the higher order finite difference schemes [26]. For the 4-th neighborhood interaction, three ghost atoms are needed on each end. From left to right, we label the left ghost atoms by $\bar{2},\bar{1},0$ and the right ones by $N+2,N+3,N+4$, respectively. Since the deformation is homogeneous in the elastic regime, i.e., the deformation gradient is a constant, we have

$$u_i = \frac{\delta}{N}(i-1), \quad i=1,2,\cdots,N+1,$$

and the discrete deformation gradient is given by

$$\frac{u_{i+1}-u_i}{x_{i+1}-x_i} = \frac{\delta/N}{r^*} = \delta, \quad i=1,2,\cdots,N.$$

Therefore, the displacement of the 0-th atom satisfies

$$\frac{u_1-u_0}{x_1-x_0} = \delta,$$

which yields $u_0 = -\delta r^*$ since $x_0 = -r^*$. The position of the 0-th atom is

$$y_0 = x_0+u_0 = -\big(1+\delta\big)r^*.$$

The same argument gives the positions of the $\bar{2}$-th, $\bar{1}$-th, $(N+2)$-th, $(N+3)$-th and $(N+4)$-th atoms as follows.

$$\begin{aligned} y_{\bar{2}} &= -3\big(1+\delta\big)r^*, & y_{\bar{1}} &= -2\big(1+\delta\big)r^*, \\ y_{N+2} &= (N+1)\big(1+\delta\big)r^*, & y_{N+3} &= (N+2)\big(1+\delta\big)r^*, \\ y_{N+4} &= (N+3)\big(1+\delta\big)r^*. \end{aligned}$$

We take the undeformed state as the initial guess of Newton method, i.e.,

$$x_i = (i-1)r^*, \quad i=2,\ldots,N.$$

Neighbors	$1-$st	$2-$nd	$3-$rd	$4-$th	Ideal
δ_c	.0105	.0108	.0109	.0109	.1086

Table 2: Numerical ideal strain vs. interaction range in MM.

Let $N=100$, and we show δ_c for different interaction ranges in Table 2. It is well-known that the number of minima decreases as the interaction range increases [8]. However, it follows from Table 2 that δ_c does not change up to the $4-$th neighbor interaction. Therefore, we consider the $4-$th neighbor interaction for this example.

Adopting different number of atoms, we obtain δ_c in terms of N. Table 3 shows that the numerical ideal strain becomes smaller as the number of atoms increases and the ideal strain is about one percent when N is larger than 1000. This is similar to the situation in the continuum model as shown in Table 1.

N	8	32	100	1024	Ideal
δ_c	.0628	.0250	.0109	.0017	0.1086

Table 3: Numerical ideal strain vs. number of atoms in MM.

We have revealed the difficulty in solving the atomistic and continuum models. In both cases, parameters must be tuned oftentimes to ensure the convergence. Moreover, the larger the number of atoms, the more the number of iterations. This is in accordance with the fact that if the number of atoms increases the problem becomes more and more intractable since more and more local minima come in. Even worse, it follows from Tables 1 and 3 that neither of them gives the feasible ideal strain.

2.3 Multigrid-like method

Consider a nested sequence of triangulations $\mathcal{T}_0 \subset \mathcal{T}_1 \subset \cdots \subset \mathcal{T}_l$ of Ω, which may be constructed by the bisection procedure. Let T be an element in $\mathcal{T}_i$. The mesh size $h_i \equiv \max_{T\in\mathcal{T}_i} \mathrm{diam} T$ satisfies

$$h_i = h_{i-1}/2 \quad \text{for} \quad i=1,\cdots,l.$$

The associated finite element spaces X_i are also nested

$$X_0 \subset X_1 \subset \cdots \subset X_l.$$

Our method is described as follows.

Step 1 Initialization: let $\boldsymbol{u}_0 = \mathbf{0}$ be the initial guess. Minimize the CB elasticity problem (2.2) discretized on $\mathcal{T}_0$ to obtain $\tilde{\boldsymbol{u}}_0$.

Step 2 For $i=1,\cdots,l$,

1. Interpolate
$$\boldsymbol{u}_i = I_{i-1}^{i} \tilde{\boldsymbol{u}}_{i-1},$$
where I_{i-1}^{i} is the standard finite element interpolation operator.
2. Let $\boldsymbol{u}_i$ be the initial guess. Minimize the CB elasticity problem (2.2) discretized on $\mathcal{T}_i$ to obtain $\tilde{\boldsymbol{u}}_i$.

Step 3 Relaxation: define the CB state as $\boldsymbol{y}_{\mathrm{CB}} \equiv \boldsymbol{x} + \tilde{\boldsymbol{u}}_l(\boldsymbol{x})$ and solve MM (2.1) with $\boldsymbol{y}_{\mathrm{CB}}$ as the initial guess.

Figure 2 is the schematic illustration of the proposed method. It is worth mentioning that the first two steps in solving the CB elasticity problem are in the same spirit of the so-called Cascadic multigrid method in [7].

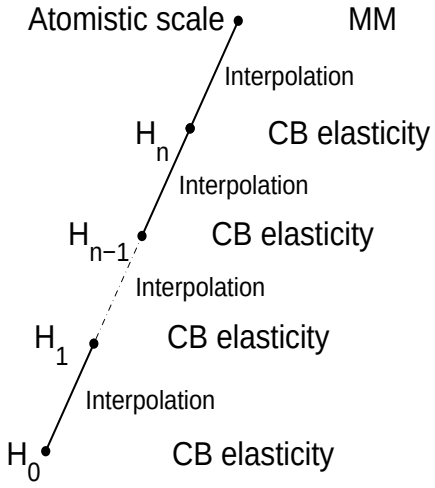

Figure 2: Schematic illustration of our method.

2.4 Comparison between our method and MM

We revisit one dimensional chain described in § 2.2. Let the number of atoms be 17, and the displacement of the left-most atom and the right-most atom be 0 and 0.05, respectively. As to MM, we generate the initial configuration of the internal atoms by the normal distribution with expectation 0 and variance 0.2. As to the proposed method, we use the initial value of the $9-$th (middle) atom in MM as the initial guess on the coarsest mesh.

First we show the total energy of the system in Figure 3 for 50 samples. If the minimization process for solving MM does not converge for a fixed number of iterations (200 in this example), or blows up, we set the energy as 0 (denoted by ∇). It is clear that the

system energy in our method keeps unchanged, while that in MM varies dramatically with different initial guesses.

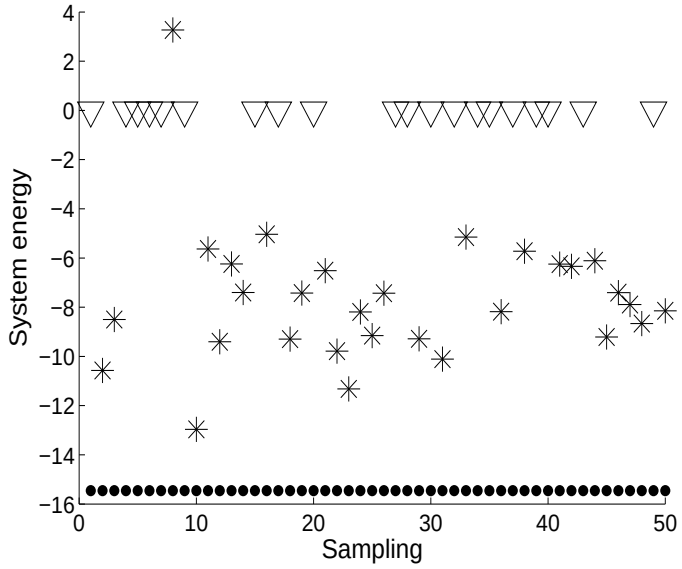

Figure 3: Energy distribution with random initial guesses. Our method $=\bullet$; MM $=*$.

Next we demonstrate that our method can give the physically relevant local minimum while MM cannot. Configurations obtained by our method for different initial guesses are the same, which explains the invariance of the system energy as shown in Figure 3. However, different initial guesses give different configurations in MM. Denote by $\bullet$ the positions of atoms in the undeformed state. We show the configuration by our method and also one configuration randomly chosen from those obtained by MM. The corresponding positions of atoms are marked by $\bigcirc$ and $\Diamond$, respectively; see Figure 4. We also present the atomic configuration of the deformed state (denoted by $\square$) obtained by MM with the undeformed state as the initial guess. The energies corresponding to $\bigcirc$, $\Diamond$ and $\square$ are -15.4575, -8.4984 and -15.5492, respectively. Since the elastically deformed state in this problem is known, a direct calculation gives that the system energy is -15.4575. We observe that our method gives exactly the elastically deformed state, which is only a local minimum of the total energy because its energy is higher than that in the $\square$ state.

Two problems arise when we solve MM directly. Firstly the energy landscape becomes more and more complex as N increases. Many attraction basins are sitting between the initial guess and the elastically deformed state. It is demonstrated in [9] that the number of local minima is expected to grow exponentially as the number of atoms increases. Under such circumstances the elastically deformed state is difficult to be captured as shown in § 2.2 and this subsection. Secondly the computational cost has the

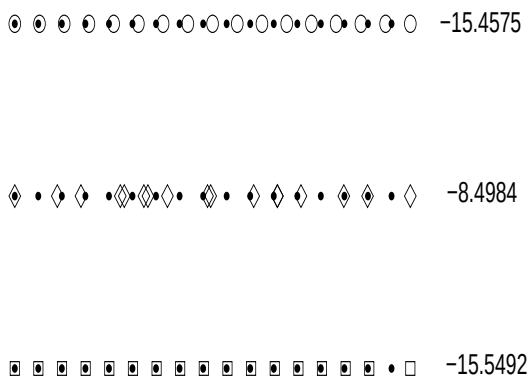

Figure 4: Atomic configurations and system energies for different methods.

superlinear growth, which will be explained in the next section.

E and Ming [12] proved that the CB elasticity model is consistent with MM under certain stability conditions, which is the theoretical foundation of the current method. The hierarchical structure is employed in the implementation, which brings out two advantages. On the one hand, the method can automatically bypass many local minima and is insensitive to the choice of the initial guess and parameters in the iterative solvers. Due to the hierarchical structure, only two kinds of minima survive finally: 1) the CB state; 2) minima around the CB state. The number of the local minima in the CB elasticity model grows exponentially as n (Dofs) increases, similar to the case in MM [9]. Therefore, the number of local minima is $\mathcal{O}(n!)$ in our method while $\mathcal{O}(N!)$ in MM. When n is small, the elastically deformed state can be easily captured. On the other hand, the current method is an $\mathcal{O}(N)$ method as shown in the next section.

3 Homogeneous Deformation

We adopt the definition of linear-scaling complexity from [19]. If CPU time of the method scales linearly in terms of the system size, i.e.,

$$T_{CPU} = CN$$

with a constant C independent of N, we call the method linear-scaling, or $\mathcal{O}(N)$ equivalently.

If only short-range interactions are considered, the cost for computing the forces on each atom scales $\mathcal{O}(N)$. One may think that $\mathcal{O}(N)$ methods emerge naturally for solving

MM in this case. Actually this is not true. We always encounter problems with strong nonlinearity in MM. When this kind of problems are solved iteratively, we cannot guarantee that the number of iterations does not increase as the system size increases. Take the elastically deformed state as an illustrative example. This state is smooth and can be generated by the collective motion of all atoms in the system. Roughly speaking, to generate the collective motion, the number of iterations is at least $\mathcal{O}(N)$ since one step iteration can only update positions of atoms up to certain neighbors. Therefore, even if only short-range interactions are considered and an $\mathcal{O}(N)$ solver is employed for linear systems at each step, the total cost for generating the elastically deformed state scales at least $\mathcal{O}(N^2)$. Similar phenomena have been observed in electronic structure calculations [1].

When we investigate the linear-scaling property of the method in what follows, we always extract one state from the stress-strain curve and count the total CPU time when enlarging the system size of the state. For all the examples in this section and in § 4.1, the total CPU time is recorded on LSSC-II with one Intel 2GHz Xeon processor as a measure of the computational cost.

3.1 One dimensional chain revisited

We firstly simulate one dimensional chain with the proposed method. The setup is the same as that in § 2.2. Newton method *without* line search is used for the minimization problems arising from both the CB elasticity model and MM. The resulting linear systems are solved by a parallel sparse direct solver *MUMPS* [30]. The Hessian matrices arising from the CB elasticity model are tridiagonal matrices; those arising from MM are ninth-diagonal matrices since only up to the 4-th neighbor interaction is taken into account. The computational complexity of MUMPS for solving such linear equations is $\mathcal{O}(N)$.

The stress-strain curve is plotted in Figure 5. The numerical ideal strain δ_c is 0.1086, exactly the same as the ideal strain. Before δ_c, the stress-strain curve of our method coincides with that of elastically deformed states perfectly. We also obtain the plot of the total CPU time in terms of the system size in Figure 6, which suggests that our method is linear-scaling.

3.2 Tension and shear for aluminum

Next we study the deformation of aluminum (Al) under tensile and shear loading. The atoms are assumed to be interacting through the embedded-atom method (EAM) potential [6] of the form:

$$E = \frac{1}{2}\sum_{i,j}\phi_{ij}(r_{ij}) + \sum_i U_i\Big[\sum_j \rho_i(r_{ij})\Big],$$

where ϕ_{ij} is the pairwise potential, r_{ij} is the distance between the i-th and j-th atoms, U_i is the glue function and ρ_i is the atomic density function of the i-th atom. Parameters in the potential function are taken from [15] and we refer to [34] for the expression of W_{CB}

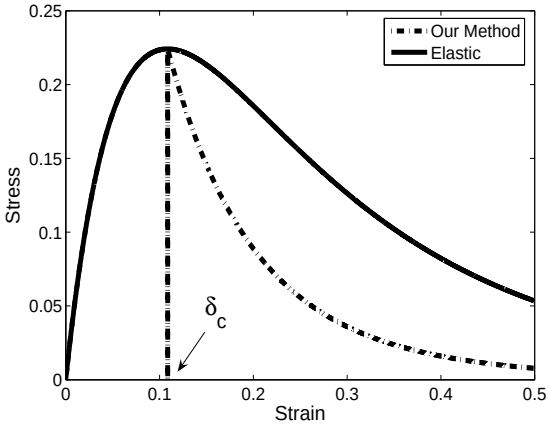

Figure 5: Stress-strain curve for one dimensional chain.

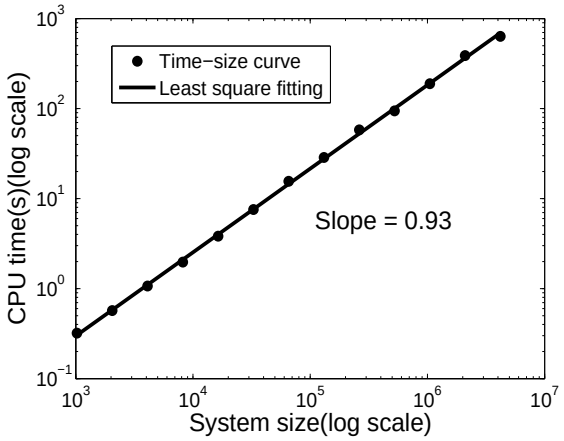

Figure 6: CPU time vs. system size for one dimensional chain (Log-log plot).

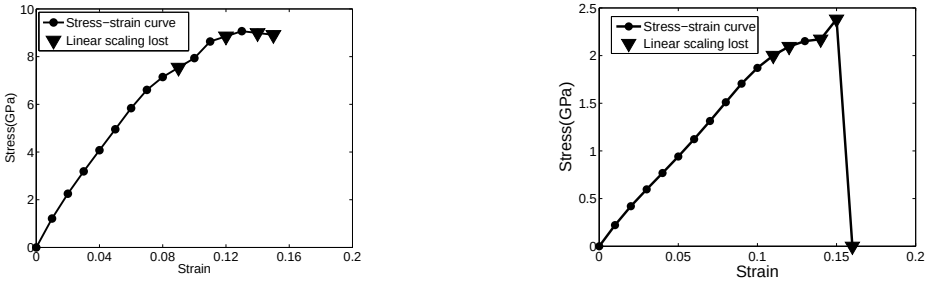

Figure 7: Stress-strain curves for Al. Left: tension; Right: shear.

based on the EAM potential. The cut-off radius is $5.56\mathring{A}$ [15], which includes up to the 3-rd neighbor interaction.

We employ the CG method with Fletcher-Reeves formula and bisection line search technique [31] to solve MM. The stopping criterion is

$$\left(\frac{1}{N}\sum_{i=1}^{N}\left|\frac{\partial E}{\partial \boldsymbol{y}_k}\right|^2\right)^{1/2} < \mathrm{TOL}.$$

The CB elasticity model is approximated by hexahedral element with the standard eight-point Gauss numerical integration scheme. The resulting minimization problem is solved by the Newton-Raphson method with line search [13]. The stop criterion is

$$\left(\frac{1}{|\Omega|}\int_{\Omega}|\nabla E|^2 \mathrm{d}\boldsymbol{x}\right)^{1/2} < \mathrm{TOL}.$$

We test tension in $[111]$ (principal) direction and shear in $[11\bar{2}](111)$ direction, and set the tolerance as $\mathrm{TOL} = 1E-8$. The $[11\bar{2}]$, $[\bar{1}10]$ and $[111]$ directions are chosen as x, y and z axis, respectively. We impose Dirichlet boundary condition on z direction, while periodic boundary condition on the other two directions. Ghost atoms are introduced in z direction as that in one dimensional case. The Hessian matrices arising from this test are still sparse but not in n-diagonal form. Therefore, we replace the solver *MUMPS* by *BoomerAMG* [20] which is a linear-scaling iterative solver.

For both cases, we plot the stress-strain curves in Figure 7. The linear-scaling property is preserved at • but lost at ▼. To clarify this point, we extract one step marked by • from the curves and report the log-log plot of CPU time in terms of the system size in Figure 8, which shows that our method is indeed linear-scaling for both tensile and shear deformation. At ▼, the loss of linear-scaling property is triggered by elastic instability of the perfect crystal at finite strain as suggested in [25] and rigorously proved in [12].

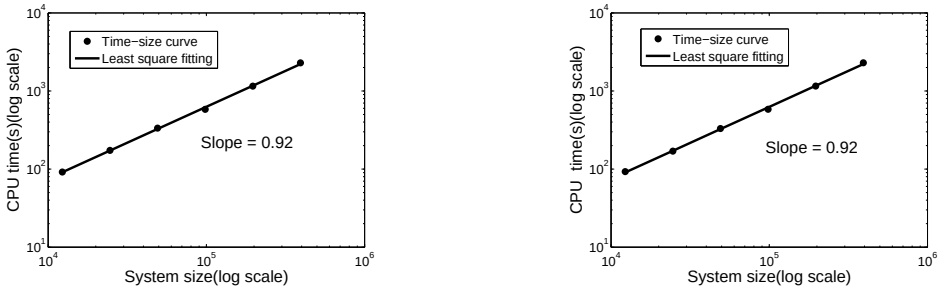

Figure 8: CPU time vs. system size for Al (Log-log plot). Left: tension; Right: shear.

4 Inhomogeneous Deformation

4.1 Vacancy

Consider a system including 196608 Al atoms interacting through EAM potential with an atom missing at the center. The occupied domain Ω is approximately $158.0\mathring{A} \times 91.2\mathring{A} \times 223.5\mathring{A}$. Let the displacement for the right-most layer of atoms in $[111]$ direction be $2.235\mathring{A}$ and that for the left-most layer of atoms be 0.

We firstly use the proposed method to study this example. The number of iterations on each level of the nested meshes can be found in Table 4. Most of the cost is spent

Level	Coarsest	Internal	Atomistic
Iteration number	17	1	14

Table 4: Iteration numbers on different levels with the current method.

on the atomistic level. Moreover, the number of iterations increases dramatically as the number of atoms increases, which implies our method is not linear-scaling any more. In order to understand the result, we plot the component of $\boldsymbol{y}_{\mathrm{CB}} - \boldsymbol{y}$ in the $[111]$ direction in Figure 9, and find that the error is localized. Based on this observation, we introduce a local correction step into the method.

The modified method is described as follows.

Step 1 Compute $\boldsymbol{y}_{\mathrm{CB}}$ by the CB elasticity model over the whole domain Ω.

Step 2 Choose a box Ω_{box} around the void. Fix atoms outside Ω_{box} and minimize MM over Ω_{box} with $\boldsymbol{y}_{\mathrm{CB}}$ as the initial guess to obtain $\widetilde{\boldsymbol{y}}_{\mathrm{local}}$.

Step 3 Define

$$\widetilde{\boldsymbol{y}} = \begin{cases} \boldsymbol{y}_{\mathrm{CB}} & \text{outside } \Omega_{\mathrm{box}}, \\ \widetilde{\boldsymbol{y}}_{\mathrm{local}} & \text{inside } \Omega_{\mathrm{box}}, \end{cases}$$

and minimize MM with $\widetilde{\boldsymbol{y}}$ as the initial guess over Ω.

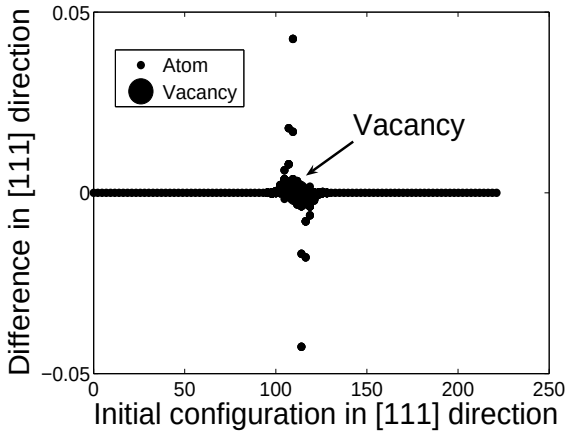

Figure 9: Difference between the CB elasticity and MM in $[111]$ direction.

In the simulation, the center of Ω_{box} is the void and Ω_{box} contains 17 layers of atoms in each direction. In Table 5, we report the number of iterations on each level with the modified method. We did not solve MM after the local correction step since $\widetilde{y}$ satisfies the stopping criterion. This means that the solution of the CB elasticity model is still a good initial guess for MM except in the box, since the influence of the void is localized and the system is still elastically deformed. We show the log-log plot of CPU time versus the system size in Figure 10 and conclude that the method is still linear-scaling.

Level	Coarsest	Internal	Local correction	Atomistic
Iteration number	17	1	15	0

Table 5: Iteration numbers on different levels with additional local correction.

4.2 Nanoindentation

In this subsection, the method is employed to study the nanoindentation problem. Consider a system with 24576 Al atoms interacting through EAM potential. The domain Ω is approximately $55.9\mathring{A} \times 39.5\mathring{A} \times 182.5\mathring{A}$. The width of the indenter is $6.98\mathring{A}$. The setup is similar to that in [33]. We simulate the nanoindentation process of Al in $[\bar{1}10]$ (dislocation) direction with a rectangular indenter (Figure 11). The $[111]$,$[11\bar{2}]$ and $[\bar{1}10]$ directions are chosen as x,y and z axis, respectively. We impose periodic boundary condition on both x and y directions, while Dirichlet boundary condition on the top surface under the indenter and the bottom surface in z direction, and Neumann boundary condition on the remaining part of the top surface.

We plot the load-displacement curve for nanoindentation in Figure 12. To illustrate the generation of dislocation, we choose an ellipse over the region where the slope of the curve is noticeably changed. After zooming in, we select four representative points

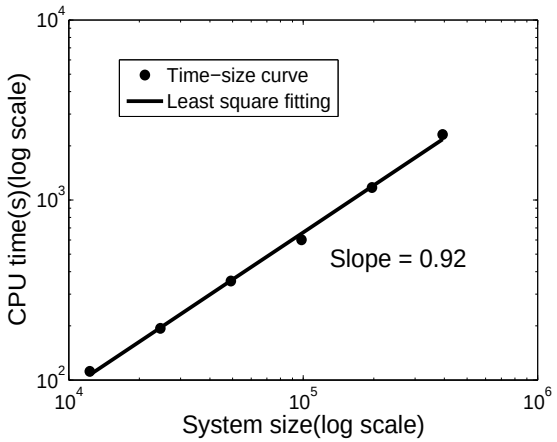

Figure 10: CPU time vs. system size for vacancy (Log-log plot).

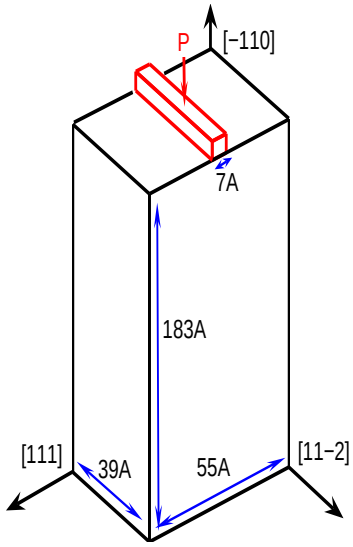

Figure 11: Schematic representation of nanoindentation along dislocation direction.

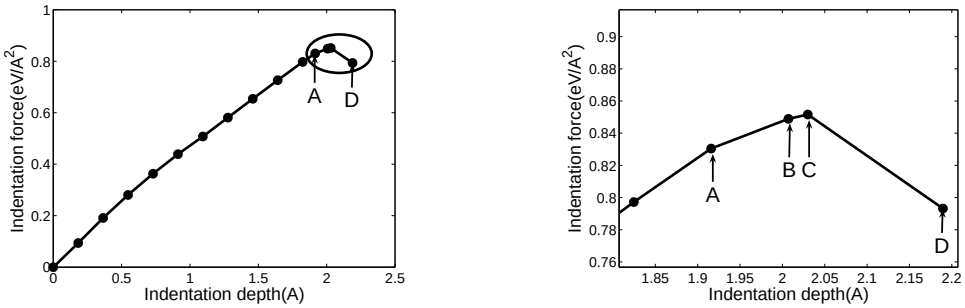

Figure 12: Load-displacement curve for nanoindentation. Left: full picture; Right: local picture after zooming in the ellipse.

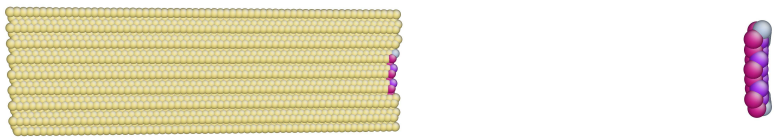

Figure 13: Atomic configuration of state A. Left: full configuration; Right: irregular atoms.

labeled by A, B, C and D sequentially, among which C is the transition point with the largest value of load. We visualize the atomic configuration by Atomeye [24] for state A,B,C and D in Figures 13– 16, respectively. We name the number of atoms touching the given atom as its coordinate number. For an ideal face-centered cubic crystal, the ones with coordinate number 12 are called regular atoms, while the others are called irregular atoms. Especially, the coordinate number of atoms associated with the dislocation here is 13. To make the generation of dislocation clearer, we shall also show the configurations by omitting the regular atoms but only reserving the irregular ones. There is no dislocation for state A. Dislocation has occurred from state B. At state C, dislocation grows but still sticks to the indenter. Dislocation leaves the indenter and propagates along the dislocation direction at state D. Before the load-displacement curve decreases, dislocation indeed occurred (state B). Therefore, one cannot decide the onset of plasticity by this curve. This study reveals the deficiency of the commonly used criterion for dislocation nucleation, and it is conforming with the experiment result in [29] and the numerical result based on cylindrical indenter in [22], although the system we test here is small.

In our simulation, the iteration number of Newton method for the CB elasticity model is smaller than 2. Table 6 shows the iteration number of CG method for MM. This problem has local singularity around the indenter. Since state C has the strongest singularity, the

Figure 14: Atomic configuration of state B. Left: irregular atoms; Right: atoms with coordinate number 13.

Figure 15: Atomic configuration of state C. Left: irregular atoms; Right: atoms with coordinate number 13.

Figure 16: Atomic configuration of state D. Left: irregular atoms; Right: atoms with coordinate number 13.

largest iteration number is required. While the dislocation leaves the indenter, it carries away certain plasticity and the singularity is weakened. This explains the fact that the iteration number at state D is smaller than that at state C.

Displacement($\mathring{A}$)	0.55	1.64	1.91(A)	2.00(B)	2.03(C)	2.55(D)
Iteration number	70	138	342	341	1825	911

Table 6: Iteration number of CG method vs. displacement.

5 Conclusion

In this work, we presented an efficient multigrid method to solve the molecular mechanics model of atomic solids. The method exhibits linear-scaling computational complexity for the problems under homogeneous deformations, and is insensitive to parameters of iterative solvers. Moreover, it automatically surmounts many unphysical local minima due to the hierarchical structure of the algorithm. Our method also works for problems with localized defects by including a correction step. However, the method is not so efficient for dislocation due to its nonlocality [27], while it is still qualitatively in agreement with the experiment results.

The present method is under development to broaden its versatility. For instance, it is straightforward to test the critical mechanical response of the crystalline solids with complex lattice structure because the consistency between the CB elasticity model and the molecular mechanics model has been proved in [12]. Further work will involve extensions to problems with point defects, dislocations and grain boundaries, molecular systems and problems at finite temperature. The first step may be a systematic study of the continuum models associated with the molecular system of interest. The Cauchy-Born elasticity model has to be modified to include more ingredients that account for the effect of the defects, since the Cauchy-Born elasticity model only applies to perfect crystal as shown in [12]. More efforts are also devoted to incorporate the present method with more sophisticate multigrid machinery to improve the efficiency when problems with the inhomogeneous deformation are considered; see cf. [28].

Acknowledgements

We thank Weinan E for inspiring discussions on the topic studied here. The work of Ming was supported by National Natural Science Foundation of China under the grants 10871197 and 10932011.

References

[1] J.F. Annett, *Efficiency of algorithms for Kohn-Sham density functional theory*, Comput. Mater. Sci., 4(1995), 23–42.

[2] X. Blanc, C. Le Bris and P.-L. Lions, *From molecular models to continuum mechanics*, Arch. Rational Mech. Anal., 164(2002), 341–381.

[3] M. Born and K. Huang, *Dynamical Theory of Crystal Lattices*, Oxford University Press, 1954.

[4] J.Q. Broughton, F.F. Abraham, N. Bernstein and E. Kaxiras, *Concurrent coupling of length scales: methodology and application*, Phys. Rev. B, 60(1999), 2391–2403.

[5] M. Chipot and D. Kinderlehrer, *Equilibrium configurations of crystals*, Arch. Rational Mech. Anal., 103(1988), 237–277.

[6] M.S. Daw and M.I. Baskes, *Embedded-atom-method: Derivation and application to impurities, surfaces and other defects in metals*, Phys. Rev. B, 29(1984), 6443–6453.

[7] P. Deuflhard, P. Leinen and H. Yserentant, *Concepts of an adaptive hierarchical finite element code*, IMPACT Comput. Sci. Engrg., 1(1989), 3–35.

[8] J.P.K. Doye, D.J. Wales and R.S. Berry, *The effect of the range of the potential on the structures of clusters*, J. Chem. Phys., 103(1995), 4234–4249.

[9] J.P.K. Doye, M.A. Miller and D.J. Wales, *Evolution of the potential energy surface with size for Lennard-Jones clusters*, J. Chem. Phys., 111(1999), 8417–8428.

[10] W. E and B. Engquist, *The heterogeneous multiscale methods*, Comm. Math. Sci., 1(2003), 87–132.

[11] W. E and P.B. Ming, *Analysis of multiscale methods*, J. Comput. Math., 22(2004), 210–219.

[12] W. E and P.B. Ming, *Cauchy-Born rule and the stability of crystalline solids: Static Problems*, Arch. Rational Mech. Anal., 183(2007), 241–297.

[13] S.C. Eisenstat and H.F. Walker, *Choosing the forcing terms in an inexact Newton method*, SIAM J. Sci. Comput., 17(1996), 16–32.

[14] P. Engel, *Geometric Crystallography: An Axiomatix Introduction to Crystallography*, D. Reidel Publishing Company, Dordrecht, Holland, 1986.

[15] F. Ercolessi and J.B. Adams, *Interatomic potentials from first-principles calculations: the force-matching method*, Europhys. Lett., 26(1994), 583–588.

[16] J.L. Ericksen, *The Cauchy and Born hypothesis for crystals*, In: *Phase Transformations and Material Instabilities in Solids*. Gurtin, M.E. (ed.). Academic Press, 1984, 61–77.

[17] I. Fonseca, *The lower quasiconvex envelop of the stored energy for an elastic crystal*, J. Math. Pures et Appl., 67(1988), 175–195.

[18] G. Friesecke and F. Theil, *Validity and failure of the Cauchy-Born hypothesis in a two-dimensional mass-spring lattice*, J. Nonlinear Sci., 12(2002), 445–478.

[19] S. Goedecker, *Linear scaling electronic structure methods*, Rev. Mod. Phys., 71(1999), 1085–1123.

[20] Hypre: a library of high performance preconditioners that features parallel multigrid methods for structured and unstructured grid problems: *https://computation.llnl.gov/casc/linear_solvers/sls_hypre.html*.

[21] P.N. Keating, *Effect of invariance requirements on the elastic strain energy of crystals with application to the diamond structure*, Phys. Rev., 145(1966), 637–645.

[22] J. Knap and M. Ortiz, *Effect of indenter-radius size on Au(001) nanoindentation*, Phys. Rev. Lett., 90(2003), 226102.

[23] J.E. Lennard-Jones, *On the determination of molecular fields. II. from the equation of state of a gas*, Proc. Roy. Soc. London Ser. A, 106(1924), 463–477.

[24] J. Li, AtomEye: an efficient atomistic configuration viewer, Model. Simul. Mater. Sci. Eng., 11(2003), 173–177.

[25] J. Li, K.J. Van Vliet, T. Zhu, S. Yip and S. Suresh, *Atomistic mechanisms governing the elastic limit and incipient plasticity*, Nature, 418(2002), 307–310.
[26] G.I. Marchuk and V.V. Shaidurov, *Difference methods and their extrapolations*, Springer, New York Berlin Heidelberg, 1983.
[27] R. Miller and D. Rodney, *On the nonlocal nature of dislocation nucleation during nanoindentation*, J. Mech. Phys. Solids, 56(2008), 1203–1223.
[28] P.B. Ming, J. Chen and Jerry Z. Yang *A constrained Cauchy-Born elasticity accelerated multigrid method for nanoindentation problems*, preprint, 2010.
[29] A.M. Minor, S.A.S. Asif, Z.W. Shan, E.A. Stach, E. Cyrankowski, T.J. Wyrobek and O.L. Warren, *A new view of the onset of plasticity during the nanoindentation of aluminium*, Nature Materials, 5(2006), 697–702.
[30] MUMPS: a parallel sparse direct solver: *http://graal.ens-lyon.fr/MUMPS/*.
[31] J. Nocedal and S. Wright, *Numerical Optimization*, Springer-Verlag, 2nd ed., 2006.
[32] G. Sih and H. Liebowitz, *Mathematical theories of brittle fracture*, in Fracture: An Advanced Treatise, Mathematical Fundamentals, H. Liebowitz ed, Academic Press, New York, 1968, 67–190.
[33] E.B. Tadmor, R. Miller and R. Phillips, *Nanoindentation and incipient plasticity*, J. Mater. Res., 14(1999), 2233–2250.
[34] E.B. Tadmor, M. Ortiz and R. Phillips, *Quasicontinuum analysis of defects in solids*, Phil. Mag. A, 73(1996), 1529–1563.
[35] E.B. Tadmor, G.S. Smith, N. Bernstein and E. Kaxiras, *Mixed finite element and atomistic formulation for complex crystals*, Phys. Rev. B., 59(1999), 235–245.
[36] Thomas C.T. Ting, *Anisotropic Elasticity: Theory and Applicatoins*, Oxford University Press, 1996.
[37] U. Trottenberg, C.W. Oosterlee and A. Schüller, *Multigrid*, Academic Press Inc., San Diego, CA, 2001, with contributions by A. Brandt, P. Oswald and K. Stüben.
[38] L. Truskinovsky, *Fracture as a phase transition*, In Comtemporary Resaerch in the Mechanics and Mathematics of Materials, R.C. Batra and M.F. Beatty eds., © CIMNE, Barcelona, 1996, 322–332.
[39] A. Yavari, M. Ortiz and K. Bhattacharya, *A theory of anharmonic lattice statics for analysis of defective crytsals*, J. Elasticity, 86(2007), 41–83.